Review Article | *Peer Reviewed* | *Open Access*

Methodological Approaches to Optical Disc and Optical Cup Segmentation: A Critical Assessment

Deepti Sahu and Mandeep Kaur*

Department of Computer Science and Engineering, Sharda University, Greater Noida, India
E-mail/Orcid Id:

DS, ✉ dmpct10@gmail.com, 🆔 https://orcid.org/0000-0001-9839-8210;
MS, ✉ drmandeepkaur10@gmail.com, 🆔 https://orcid.org/0000-0001-5163-4001

Abstract: A progressive optic nerve condition called glaucoma causes irreversible eyesight loss. Retinal fundus imaging has been used in recent years to diagnose retinal diseases. Analyzing these images effectively requires pinpointing the areas of interest, which can be tricky due to fundus images' anatomy and vascular patterns. Different image segmentation techniques are used to extract the area of interest from the fundus images. This paper explores the various segmentation methodologies, emphasizing conventional and modern retinal fundus image segmentation approaches. Evaluation measures such as the Disc damage likelihood scale, Inferior superior temporal region, Dice similarity coefficient, Jaccard index, Sensitivity and Specificity are used to measure the effectiveness of segmentation algorithms, which detect small structural changes that indicate glaucomatous damage. Furthermore, this paper also provides a detailed analysis of deep learning algorithms used for optic cup and optic disc segmentation. It shows that the deep learning model achieved higher accuracy on small datasets, but the accuracy percent is degraded on larger datasets. This detailed analysis demonstrates that accurate disc and cup segmentation remains a significant challenge and suggests that effective segmentation strategies and deep learning approaches are required for vast and complex datasets.

Introduction

Medical imaging is the technique used to generate visual representations of interior structures of the human body for diagnostic purposes. This term covers various technologies used to diagnose the human body, to monitor the human body and to treat medical conditions. Medical imaging is a multidisciplinary field that includes machine learning, computer vision, and image processing (Elyan et al., 2022). It plays a vital role in various areas of medical research, including ophthalmology. The optic nerve serves as the pathway for transmitting signals from the eye to the brain. Glaucoma is an eye disease that causes damage to the optic nerve. Such damage disrupts signal transmission to the brain, potentially resulting in blindness. As per a survey conducted by WHO, the prevalence of glaucoma, an age-related eye condition, is projected to increase by 1.3 times from 76 million in 2020 to 95.4 million by 2030. Figure 1 illustrates the estimated global population affected by degeneration and glaucoma according to the WHO survey (2022). According to Prevalence surveys, 111.8 million people worldwide will suffer from glaucoma by 2040 (Tham et al., 2014).

Glaucoma is a progressive eye disease which can be identified by analyzing damages in the optic nerve; this is the leading cause of irreversible vision loss if untreated. Elevated intraocular pressure (IOP), also known as ocular hypertension, is responsible for this damage. When the eye's fluid does not drain properly, it creates high IOP inside the eye and damages the optic nerve head, and the result is abnormal optic cup and disc size. The peripheral neuro-retinal rim and the bright central optic cup are the two zones that form the optic disc in fundus imaging (Govindan et al., 2024). All people possess optic disc (OD) and cup. However, abnormal cup and disc size shows glaucoma. The abnormal size of the optic cup and optic disc can be evaluated using the cup-to-disc ratio (CDR).
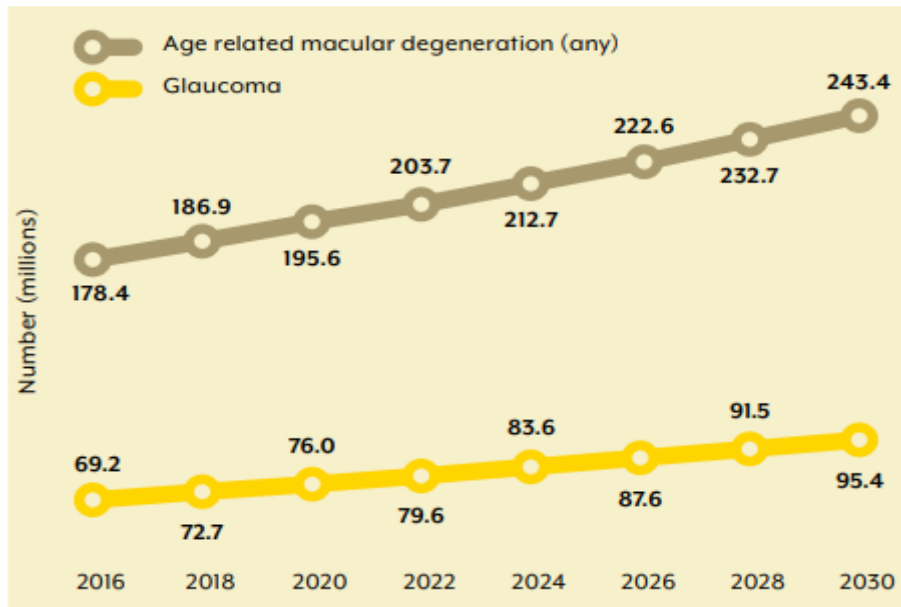
Figure 1. Estimated global population affected by age-related macular degeneration and glaucoma.

The CDR ranges from 0.1 mm to 0.9 mm, 0.5 mm or more CDR value is seen as indicative of glaucoma. If it is less than 0.5 mm, CDR is considered normal.

of low drainage and low aqueous humor, production may be the cause of glaucoma. Table 1 shows the relationship between IOP and the Eye fluid drainage system.

Figure 2. Glaucoma Risk Factor.

High intraocular pressure depends on the drainage capability of the aqueous humor drainage system inside the eye (Gupta et al., 2021). This system depends on genetic predispositions and age-related changes. High aqueous humor production and high intraocular pressure depend on the drainage capability of the drainage system of aqueous humor inside the eye (Gupta et al., 2021). This system depends on genetic predispositions and age-related changes. High aqueous humor production and high drainage lead to no IOP, high aqueous humor production and low drainage lead to high IOP, Low aqueous humor production and high drainage lead to No IOP and in case

Other reasons for glaucoma include ethnicity (certain ethnic groups, such as African Americans and people of Asian descent, have a higher risk of developing glaucoma and high intraocular pressure), eye conditions like uveitis, certain medical conditions such as diabetes, and some medications like corticosteroids (Delgado et al., 2019; Una et al., 2019). Figure 2 shows the major risk factors of glaucoma.

In recent years, a combination of computer vision techniques and clinical attributes of fundus images like an optic cup, optic disc, ISNT, etc. have been employed to effectively detect and monitor glaucoma. Prominent computer vision techniques like object detection, semant-

Table 1. Relation between IOP and eye fluid drainage system.

Drainage	Aqueous Humor Production	
	High	**Low**
High	No IOP	No IOP
Low	IOP	May be

ic segmentation, panoptic segmentation, etc. have been used for glaucoma detection. These computer vision techniques are used to analyze glaucoma using clinical attributes. Clinical attributes required for glaucoma detection include cup-to-disc ratio, disc and cup shape, RNFL thickness, blood vessel analysis, Inferior, superior nasal temporal (ISNT) rule (Sivapriya & Keerthika, 2022), etc. These attributes are important for the glaucoma detection process because they help in standardization (Automated analysis helps ensure consistency in evaluating these parameters across different exams.), quantification (Computer vision allows for objective measurement of these parameters, reducing subjectivity compared to manual assessment.), and early detection (Some parameters may be able to detect subtle changes earlier than traditional methods.). However, the accuracy of the analysis depends heavily on the quality of retinal images. Retinal images are captured through the fundus cameras; the fundus camera captures color photographs of the retina and posterior segment of the eye. These images are valuable in evaluating the structural alterations in the eye related to glaucoma. An important structural change in glaucoma is the modification in the shape of the optic disc, which is seen as a bright elliptical structure in the color fundus images, as depicted in Figure 3.
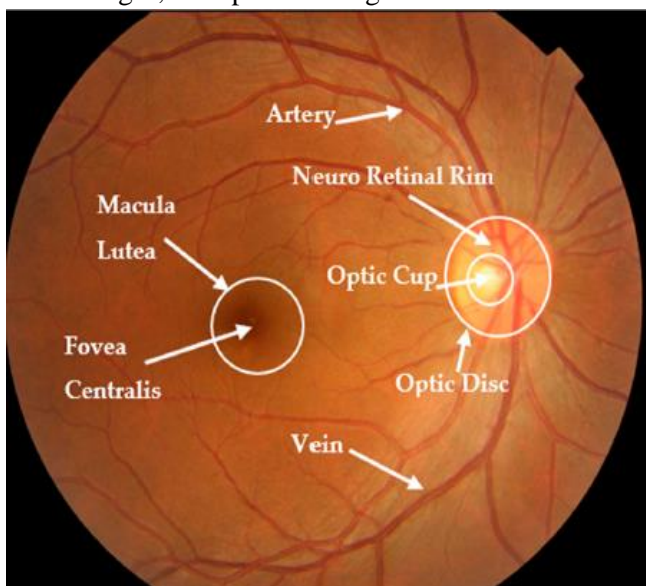
Figure 3. Anatomy of Eye Image.

Fundus imaging is now considered as an aspect of identifying and monitoring glaucoma. However, analyzing these images effectively requires pinpointing the areas of interest, which can be tricky due to fundus images'

anatomy and vascular patterns (Medhi et al., 2023). Image segmentation techniques are used to extract the region of interest from these complex images. Segmentation involves separating and outlining structures or areas of focus in an image (L. K. Singh et al., 2020). Segmentation algorithms play a role in extracting features linked to glaucoma in fundus images, such as the optic cup and optic disc. In this paper, an analysis has been done by applying different segmentation approaches to some datasets. The major contributions of this research paper are as follows:

#This paper presents a systematic review of literature in the broad domain of glaucoma detection using image segmentation and presents datasets, techniques, and evaluation measures used in this domain.

To the best of our knowledge, no work thoroughly applies different image segmentation techniques on a dataset to provide a comprehensive comparison.

The rest of this paper is structured as follows: Section 2 discusses the commonly used terminologies used for glaucoma detection using Fundus. Further, this section describes the different types of image segmentation techniques. Section 3 reviewed the existing segmentation methods used for glaucoma detection. Section 4 describes various fundus image data sets, Evaluation matrices to check the effectiveness of the glaucoma detection methods and comparative studies of deep learning-based and non-deep learning-based segmentation methods. Section 5 describes the conclusion and future scope of this study.

Background

This section discusses the preliminaries required for a better understanding of the remaining parts of this paper. This section discusses commonly used terminologies related to Fundus images and segmentation. It further provides an overview of various available image segmentation techniques.

 # Optic disc: The optic disc is the point in the eye where the optic nerve and retina meet. Visual information from the eye to the brain is transmitted through the cluster of around 1.2 million densely packed nerve cells, which creates a slightly elevated region with a central depression. A typical optic disc in a healthy eye has a diameter of around 1.5 mm and appears orange to pink, whereas a glaucomatous optic disc is pallid (Rawat & Kurmi, 2020).

 # Optic cup: The optic cup is a central depression located within the OD. It is created by the densely packed

nerve cells passing through a small eye-opening. A healthy optic nerve exhibits a tiny optic cup as a result of the presence of thick, densely packed nerve cells along its margins. In disorders such as glaucoma, the nerve cells are damaged, leading to an expansion of the optic cup. In individuals without any abnormalities, the OC size is one-third of the OD size (Sahu and Kaur, 2021).

 # Optic cup to optic disc ratio: Optic cup to optic disc ratio (CDR) evaluated as the ratio of OC length to OD length as shown in Equation 1. It is a diagnostic measure used to identify glaucoma. A high CDR value is usually indicative of optic nerve damage. Figure 2 illustrates the OD and OC within the human eye (Chan et al., 2017).

$$cdr = \frac{Area\ of\ Optic\ cup}{Area\ of\ Optic\ Disc} \qquad (1)$$

 # Retinal vessels: The arteries and veins that are near to one another are referred to as retinal vessels. Retinal vessels in fundus images play a critical role in glaucoma detection by indicating structural changes and abnormalities such as vessel thinning, occlusions, and altered blood flow patterns. Analysis of retinal vessel parameters like diameter, tortuosity, and the ISNT rule aids in early diagnosis and monitoring of glaucomatous optic nerve (Thakur and Juneja, 2021).

Segmentation Techniques

A retinal fundus image consists of multiple physiological parts; only a few parts are important in determining glaucoma. Retinal fundus image segmentation helps segregate these crucial aspects from the image. Traditionally, retinal image segmentation for glaucoma detection has relied on techniques like thresholding, edge detection, and region-based methods. These approaches often require parameter tuning and can struggle with variations in image quality and illumination. However, recent advancements have seen the rise of deep learning-based segmentation. Convolutional neural networks (CNNs) have demonstrated remarkable capabilities in accurately segmenting the OD and OC from complex retinal images. These deep learning models can learn intricate hidden patterns from large datasets and achieve impressive accuracy compared to traditional methods. Moreover, hybrid methods that combine traditional techniques with deep learning frameworks have emerged, leveraging the strengths of both approaches to achieve even greater segmentation performance. This diverse array of segmentation techniques underscores the ongoing efforts to refine glaucoma detection methods, aiming to improve patient outcomes through early diagnosis and intervention. Figure 4 shows various types of segmentation techniques.
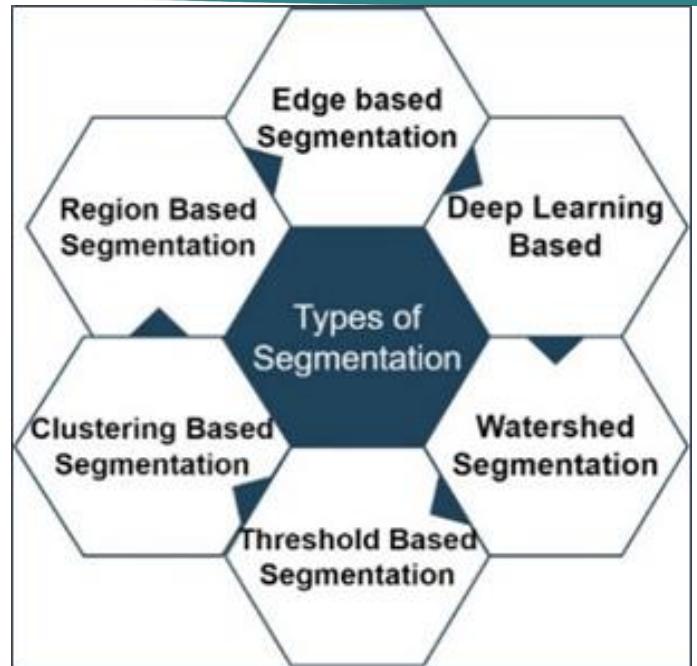

Figure 4. Types of Segmentation Techniques.

Threshold-based segmentation technique: Thresholding is a basic segmentation method employed to convert grayscale or coloured images into binary representations. This technique creates a segmented image by using a threshold value to differentiate colours below and above the threshold. Pixels are divided into partitions based on their intensity values (Chatterjee et al., 2021). The process of global thresholding involves segmenting the image into segments using Equation 2.

$$t(r,s) = \begin{cases} 1, & if\ t(r,s) > Td \\ 0, & if\ t(r,s) \le Td \end{cases} \qquad (2)$$

Here t(r, s) is the value of the binary image at the coordinates (r, s) and Td is the optimal threshold value.

When using variable thresholding, the value of T might vary across the image based on the surrounding pixels at (o,p) as given in Equation 3. However, the process of multi-thresholding involves specific thresholds, Td1 and Td2.

$$t(o,p) = \begin{cases} a, if\ f(o,p) > Td2 \\ b, if\ Td1 < f(o,p) \le Td2 \\ c, if\ f(o,p) \le Td1 \end{cases} \qquad (3)$$

Otsu's Method is a widely used technique for automatically determining the optimal threshold value in image segmentation. By maximising the pixel values between class variations, the threshold is determined. The drawbacks of the threshold-based approach include that it may not work well for images with low contrast or overlapping intensity distributions, and it is challenging to handle intricate retinal features like blood vessels.

Edge-based segmentation technique: Edge-based

segmentation in computer vision and image processing focuses on identifying and analyzing object boundaries within images by detecting edges, which are sharp changes in color or intensity that signify divisions between different sections or objects (Ilesanmi et al., 2023). The process involves two main steps: edge detection and edge linking. Common edge detection techniques include Scharr, Canny, Sobel, and Prewitt operators. Methods such as the Hough Transform or contour tracing are used to connect detected edges. Clinicians can use edge-based segmentation to enhance glaucoma diagnosis and monitoring by classifying image pixels based on texture, color, and gray discontinuities. This approach helps in feature extraction, OD and OC detection, and RNFL thickness estimation. Algorithms like Canny, Sobel, and Laplacian of Gaussian (LoG) are frequently applied in edge-based segmentation.

\# Watershed-based segmentation technique: The Watershed algorithm is used for segmenting images with touching or overlapping objects by treating the grayscale image as a topographic surface, where pixel values represent elevation (Rao et al., 2021). This method views the image as a landscape with ridges and valleys, with elevation defined by pixel grey values or gradient magnitudes. Researchers utilize this approach to partition images into distinct regions based on gradient information, accurately delineating key anatomical structures. This segmentation technique helps identify structural abnormalities associated with glaucoma, such as OD cupping and RNFL thinning, allowing for precise disease severity assessments. Additionally, it facilitates extracting quantitative measurements like disc-to-cup ratio and RNFL thickness, enhancing automated glaucoma detection systems and improving patient management.

\# Clustering-based segmentation technique: Clustering-based segmentation offers an approach to analyze images and spot changes related to the glaucoma disease. Considering factors like pixel intensity, color and texture, this method employs clustering algorithms such as k and fuzzy c means to divide the image into regions with characteristics. This process of grouping pixels into clusters assists in outlining anatomical features. These methods are beneficial in pinpointing abnormalities such as cupping of the disc (OD) or thinning of the nerve fiber layer (RNFL) (Jiang et al., 2012).

\# Label set approach-based segmentation: Topology issues that arise during the evolution of curves can be successfully resolved with the level-set method. The fundamental concept is to depict the surfaces or curves as the zero-level set of a hyper-surface with higher dimensions, manages topological change very well and

also yields more accurate numerical implementations (Saha et al., 2023). The term "level set" refers to the closed curve C with auxiliary function W that is represented in two dimensions. In Equation 4, C is regarded as the zero level of ø.

$$C = \{(o, p) | \emptyset(o, p) = 0\} \tag{4}$$

The evolution of ϕ is governed by the level set equation, as given in Equation 5.

$$\frac{\partial \phi}{\partial ti} + F|\nabla \phi| = 0 \tag{5}$$

Where: ϕ(o,p,t) is a level set function at time ti, the time derivative of ϕ is, ∇ϕ is the gradient of ϕ, and F is the speed function that controls the motion of the level set.

\# Deep learning-based segmentation technique: Deep learning-based segmentation techniques have been an advanced approach for detecting glaucoma in recent years, bringing a revolution in medical imaging. Convolutional neural networks (CNNs) are essential in deep learning to extract hierarchical features from images [24]. It can effectively identify features once it has been trained on extensive data sets of annotated retinal images. These networks capture complex spatial dependencies and image variations by using multiple convolutional layers and provide accurate and reliable segmentation. Deep learning-based methods are scalable and adaptable, enabling models to generalize across various datasets and imaging modalities(Saha et al., 2023). By using deep learning techniques, researchers can develop automated tools for early diagnosis, monitoring disease progression, and disease treatment (Ma et al., 2024).

Related Work

This section discusses the techniques used by different researchers to segment the OD and OC, as indicated in Section II. Zahoor & Fraz (2017) proposed a method for the localization of the optic disc in fundus images using a combination of the circular hough transform and a polar transform-based adaptive thresholding technique. On the MESSIDOR dataset, the method achieved 99.18% accuracy in 1.8 seconds. For the DIARETDB1 dataset, the accuracy was 99.37%, with a processing time of 1.3 seconds. The DRIONS-DB dataset yielded an accuracy of 99.86% and a processing time of 1.6 seconds. Similarly, the DRIVE dataset achieved an accuracy of 99.80% with a processing time of 1.6 seconds. Lastly, the RIM-ONE dataset resulted in an accuracy of 97.7%. However, small and imbalanced datasets may limit the generalizability and robustness of the proposed methodology. The restriction of optic disc retinal image has been removed by Sevastopolsky (2017) as their research proposes the

segmentation of optical disc and optic cup. This paper utilized a modified U-Net deep learning model with a processing time of 0.1 seconds. The performance of the proposed models was evaluated on DS and IoU. On the RIM-ONE database, the modified U-Net model achieved an impressive dice score of 0.89 and an IoU of 0.95, indicating excellent segmentation accuracy. These quality metrics are independent of class imbalance, object scale, or image scale, but the size of the data size very small.

An automated adaptive system for segmenting the optic disc using intensity-based thresholding and the optic cup via vessel bend points inside the optic disc was proposed by M. et al. (2018). The model was validated on a 225-image database with expert labels and achieved 96.85% accuracy for normal, and 95.56% accuracy for glaucoma suspect cases. The presence of bright and dark pixels around the optic disc boundary, known as peri-papillary atrophy and the small dataset size may impact segmentation accuracy and reliability. Fu, Cheng, Xu, Zhang, et al. (2018) proposed a segmentation-guided network that detects the disc from the whole fundus image. This network, including a U-net with an additional branch from the saddle layer, achieved an accuracy of 84.29% on the SCES dataset and 74.95% on the SINDI dataset. Sensitivity and specificity on the SCES dataset were 84.78% and 83.80%, respectively, while on the SINDI dataset, they were 78.76% and 71.15%. The SCES dataset contains 1,676 images and the SINDI dataset contains 5,783 images. The results indicated lower accuracy for larger datasets, influenced by peri-papillary atrophy and blood vessel interference.

Al-Bander et al. (2018) proposed a model that integrates DenseNet with a convolutional network; the method achieves pixel-wise delineation of OD and OC borders. It was evaluated on the ORIGA dataset and achieved 99.89% accuracy, 96.09% sensitivity, 99.95% specificity for OD, and 99.85% accuracy, 91.95% sensitivity, and 99.91% specificity for OC. Despite the short testing time of less than 0.5 seconds, training took 15 hours only for 455 images. Athab et al. (2019) used global and multilevel thresholding on the DRISHRHI-GS data set to segment the OD and OC, achieving 94.75% and 94.32% accuracy, respectively. Liu et al. (2019) used contrast-limited adaptive histogram equalization (CLAHE) to enhance image quality and a single-label modified U-Net model for segmenting the optic disc and cup. For this method RIGA dataset gives average dice scores of 97.31% (disc) and 87.61% (cup), DRISHTI-GS scores were 97.38% (disc) and 88.77% (cup), and RIM-ONE scores were 96.10% (disc) and 84.45% (cup). The model performance may be affected by poor-quality images since it was trained on the

high-quality RIGA dataset Yu et al. (2019). Thakur & Juneja (2019) segmented the OD and OC using a Level set Adaptively Regularized Kernel Based Intuitionistic Fuzzy C-Means (LARKIFCM), with initial manual cropping for accuracy. The method achieved OD segmentation accuracies of 94.84%, 93.23%, and 95.34% on MESSIDOR, RIM,-ONE and DRISHTHI-GS datasets and OC segmentation accuracies of 93.4% and 92.6% on RIM-ONE and DRISHTHI_GS. This project shows low OC precision in this research project.

G-net, a modified U-Net with two neural networks, achieved 95.8% accuracy for optic disc segmentation and 93% for optic cup segmentation, tested on 50 fundus camera images. The segmentation module returns the optic disc's mask Juneja et al. (2020). Juneja et al. (2020) proposed the Disc Cup Segmentation Glaucoma Network (DC-Gnet) model to extract glaucoma-related parameters and segment the optic cup and disc. Using RIM-ONE and Drishti-GS datasets, DC-Gnet achieved 97.8% accuracy on RIM-ONE and 90% on Drishti-GS. While the G-net model excels in segmentation, DC-Gnet performs better on the RIM-ONE dataset Juneja et al. (2020). A CAD model, Le-Net architecture to validate input images and the brightest spot algorithm to identify the Region of Interest (ROI) from the validated images was introduced by Shinde et al. Shinde (2021). In this work, U-Net was used for optic disc and cup segmentation on the DRIONS-DB dataset and achieved 93% accuracy for the OD and 87% for the OC. The performance of this model was affected by parapapillary atrophy.

Ganesh et al. (2021) proposed the GD-Ynet model for segmenting the optic disc and detecting glaucoma, achieving accuracies of 99.72%, 98.02%, 99.50%, and 99.41% on ACRIMA, DRISHTHI-GS, REFUGE, and RIMOne-V1 datasets, respectively. This model employs a hierarchical strategy relying on aggregated transformations and CAM to segment the ROI. The model addresses overlooked neuroretinal rim losses, disc cupping, and multiclass segmentation pathologies. Ray et al. Ray et al. (2022) introduced a mean-C thresholding method where each pixel's threshold value is determined based on local statistical measures such as the mean and median values of neighbouring pixels. This method was evaluated on the HRF-DR dataset and achieved 94.27% Sensitivity, 87.86% Specificity, and 95.61% Accuracy. The INSPIRE AVR dataset achieved 91.10% Sensitivity, 86.97% Specificity, and 95.16% Accuracy. The limited dataset size remains a persistent challenge.

Gampala et al. (2022) introduced a deep neuro-fuzzy network (DNFN) for glaucoma detection. After noise removal, the DeepJoint model segments blood vessels and

blackhole entropy fuzzy clustering locates the optic disc. The DNFN, trained with MultiVerse Rider Wave Optimization (MVRWO), classifies the final output based on the DNFN's loss function. Au-Net model was used to extract the borders of OD and OC proposed by P. et al. (2021). Sanghavi et al. Sanghavi & Kurhekar (2024) introduced a technique using Simple Linear Iterative Clustering (SLIC) and the normalized graph cut algorithm for OD segmentation, followed by a thirteen-layer CNN for classification. This method created superpixels based on color similarity and spatial proximity. The normalized graph cut algorithm then used these superpixel clusters to produce a region of interest, effectively minimizing the cut value and achieving superior image partitioning. Tadisetty et al. (2023) employed the U-Net model on various fundus datasets, using segmentation measures for performance evaluation. The canny edge detection operator is utilized for edge detection. The process includes five steps: noise reduction with Gaussian blur, gradient computation, minimum suppression, double thresholding, and edge tracking using hysteresis. The authors Sujithra & Albert Jerome (2024) proposed the ACBSS (adaptive cluster-based superpixel segmentation) technique for extracting retinal blood vessels from improved image sequences. Adaptive K-means clustering efficiently forms clusters with a precise K value using a gray-level cooccurrence matrix for feature extraction. The technique employs picture gradients for contour and texture characteristics, automatically calibrating attribute weights. Multiple iterations ensure accurate segmentation, effectively distinguishing between different pixel groups and producing favourable outcomes in the final segmentation result. Chaurasia & Culurciello (2017) proposed LinkNet to link each encoder and decoder for semantic segmentation. There is some spatial information lost in the encoder during the numerous downsampling processes. Every encoder layer's input is also bypassed to reach the output of the matching decoder to retrieve the lost data utilising residual block rather than concatenation, LinkNet additionally employs ResNet-18 as an encoder.

Research and Methodology

This section discusses the different evaluation metrics used to check how well segmentation techniques identify pertinent anatomical structures and abnormalities in retinal images. Further, various fundus image data sets and the comparative study of existing segmentation techniques are also discussed in this section.

Dataset

Commonly used datasets for glaucoma detection are DRISHTHI, RIM-ONE, REFUGE, ACRIMA, ORIGA, DRIONS-DB, HRF-DR, SECES, SINDI, PAPILA, and G1020. Table 2 shows the different datasets available for glaucoma diagnosis.

Evaluation Metrics

The performance of segmentation techniques must be evaluated to gauge how well they identify pertinent anatomical structures and abnormalities in retinal images. The effectiveness of segmentation algorithms is often assessed using several measures, including DDLS, ISNT, DSC, Jaccard index, accuracy, dice coefficient, and sensitivity.

DDLS(Disc damage likelihood scale)

The OD's damage level is measured using a grading system called the DDLS. It provides a standardized way for medical professionals to assess structural alterations in the optic nerve head. Higher scores on the scale, which normally runs from 0 to 10, indicate more severe disc injury (Zangalli et al., 2011).

Inferior superior nasal temporal (ISNT)

ISNT stands for inferior, superior, nasal, and temporal rim width sequence. The order of I, S, N, and T will increase for the aberrant eye, i.e., Inferior < superior < nasal < temporal (Maupin et al., 2020).

Dice similarity coefficient (DSC)

Segmented region and ground truth region overlap is measured using DSC. The ratio of the sum of the segmented and ground truth regions to twice the intersection of the two regions is the formula used to compute it, as shown in Equation 6. A higher DSC indicates better segmentation accuracy.

$$ds = \frac{2|DA \cap SA|}{|SA| + |DA|} \qquad (6)$$

Jaccard Index (JI)

JI, also known by the name Intersection over Union (IoU), evaluates how similar the segmented and ground truth regions are to one other. It is computed as the ratio of segmented and ground truth regions intersection and their unions. As stated in Equation 7, a greater JI value denotes superior segmentation performance (Coan et al., 2023).

$$ji = 1 - \frac{DA \cap SA}{DA \cup SA} \qquad (7)$$

Sensitivity and specificity

Sensitivity quantifies the proportion of true positive (properly segmented) points relative to all points in the ground truth, as demonstrated in Equation 8. Specificity (true negative rate) quantifies the proportion of real negative points (properly segmented background points) relative to all negative points in the ground truth as demonstrated in Equation 9. To accurately identify both

Table 2. Different datasets are used for glaucoma diagnosis.

References	Dataset	Images
Zhuo Zhang et al. (2010)	ORIGA light	Out of the 650 retinal images, 168 images are glaucomatous and Normal images are 482
Fumero et al. (2011)	RIM-ONE	It comprises 313 retinal images of normal eyes and 172 images of glaucoma patients.
Staal et al. (2004)	DRIVE	At a resolution of 584 × 565 pixels, there are 40 fundus images.
Saba et al. (2018)	DRION-DB	At a resolution of 600 × 400 pixels, There are 110 retinal images
Kauppi et al. (2007)	DIARETDB1	There are 84 fundus images of 1500 × 1152 pixels in size.
Muchuchuti & Viriri (2023)	SCES	Contains 46 glaucomatous and 1630 normal images
Sikder et al. (2019)	APTOS	3662 images
Fu et al. (2019)	REFUGE	Contains 1200 color fundus images.
Almazroa et al. (2018)	RIGA dataset	750 images
Sivaswamy et al. (2014)	DRISHTHI-GS	101 image, 70 glaucoma 31 Non glaucomic
Bajwa et al. (2020)	G1020 dataset	1020 photos, 296 from 110 patients had glaucoma, while 724 from 322 patients showed normal

the target structures and the background, it is important to evaluate the ability of a segmentation technique, including both sensitivity and specificity (Coan et al., 2023).

$$Sf = \frac{TN}{TN+FP} \qquad (8)$$

$$Sv = \frac{TP}{TP+FN} \qquad (9)$$

 # Accuracy

By computing the ratio of perfectly classified pixels to the pixels count in the image, as provided by Equation 10, accuracy assesses the overall correctness of the segmentation findings.

$$ay = \frac{Sv+Sf}{2} \qquad (10)$$

Recall, also known as sensitivity, quantifies the percentage of real positive pixels to all positive pixels in the ground truth, whereas precision measures the percentage of true positive pixels to all positive pixels in the segmented region. Recall shows how comprehensive positive predictions are, whereas precision shows how accurate positive predictions are (Thakur & Juneja, 2021).

Result and Analysis

This part extensively reviews segmentation methodologies employed in retinal image analysis during

the glaucoma detection process, from conventional to computational methods. Furthermore, the role of

evaluation matrices is examined in assessing the performance of these segmentation algorithms. Table 3 presents a comparative study of different segmentation strategies that do not employ deep learning approaches, whereas Table 4 presents a comparative study of various segmentation techniques that utilise deep learning approaches. By critically analyzing different metrics, this study aims to provide insights into their effectiveness in capturing the subtle variations associated with glaucoma in retinal images.

Using the DRISHTHI-GS dataset, figure 5 displays the accuracy percentage of the several segmentation approaches utilised from the year 2018 to 2024 to segment the optic disc. It is observed that many researchers have used the DRISHTI-GS data set for their research purposes as it provides a fair amount of malignant and benign data. However, variations exist in the performance across segmentation tasks and this paper highlights the technique-specific strengths and its use in various clinical and research contexts for the diagnosis and monitoring of glaucoma.

Table 3. comparative study on Segmentation Techniques without Deep Learning Approach.

S.N.	Authors	Approaches used for Segmentation		Performance			Data Set
		Technique Used	Approach	Measure	OD Values	OC Values	
1	M. et al., 2018	Adaptive threshold, corner threshold and Intensity-based threshold	Thresholding	Execution time	0.39 sec	0.0003 sec	Private data set
2	Athab, 2019	Global thresholding and Otsu thresholding	Thresholding	Accuracy Sensitivity Specificity	94.75% 95.06% 95.93%	94.32% 78.77% 98.48%	DRISHTI-GS
3	Thakur & Juneja, 2019	LARKIFCM	Level set-based and Clustering	Accuracy Dice similarity	94.84% 93%	93.4% 91%	RIM ONE DRISHTI-GS
4	Rao et al. (2021)	Watershed algorithm for contour shape extraction	Watershed	Dice Metric IOU Accuracy	98.76% 93.23% 98.45%	97.13% 92.10% 97.32%	DRISHTI – GS
5	Natarajan et al., 2021	fuzzy C-means algorithm	Clustering based	Accuracy Sensitivity Specificity	94.7% 95.6% 90.4%	_	DRIONS-DB
6	Pathan et al., 2021	Clustering based threshold	Thresholding	Accuracy	99.1%	97.42%	DRISHTI-GS
7	Ray et al., 2022	Mean-C thresholding	Thresholding	Accuracy Sensitivity Specificity	95.61% 94.27%, 87.86%	_	HRF-DR
8	P. B. Singh et al., 2023	Modified level set algorithm	Level set	Dice coefficient Jaccard Index	_	91.8% 75.6%	ACRIMA
9	Sanghavi & Kurhekar, 2024	Normalized graph cut algorithm and Simple linear iterative clustering	Clustering based	Accuracy Precision	96.3%	_	DRISHTI-GS1, ACRIMA, RIM-ONE R3, ORIGA, PAPILA , G1020

Table 4. Literature Survey on Deep Learning-based Segmentation Techniques.

S.N	Authors	Approaches used for segmentation		Performance Measures			Data Set
		Technique used	Approach	Measure	OD Values	OC values	
1	Sevastopolsky, 2017	Modified U-Net	Deep learning	IOU Dice Prediction time	89% 96% 0.1 sec	69% 82% 0.06 sec	RIM-ONE v.3
2	Fu et al., 2018	Modified deformable model (M-net)	Deep learning and polar transform	Accuracy	98.3%	93.0%	ORIGA and SCES datasets
3	Fu et al., 2018	DENet	Deep learning	Accuracy Specificity Sensitivity Accuracy Specificity Sensitivity	84.29% 83.80% 84.78% 74.95% 71.15% 78.76%	–	SCES SINDI
4	Al-Bander et al., 2018	FC-DenseNet	Deep learning	Dice coefficient Jaccard index Accuracy Sensitivity Specificity	96.53% 93.34% 99.89% 96.09% 99.95%	86.59% 76.88% 99.85% 91.95% 99.91%	ORIGA
5	Yu et al., 2019	U-net modified from Resnet-34	Deep learning	Dice coefficient Jaccard index Dice coefficient Jaccard index	97.38% 94.92% 96.10% 92.56%	88.77% 80.42% 84.45% 74.29%	DRISHTI-GS RIM-ONE
6	Shoukat et al., 2021	Neuroretinal area segmentation	Deep learning	Accuracy	91.25%	--	DRIHSTHI
7	Juneja et al., 2020	G-net	Deep learning	Dice metric Jaccard Index	93.6% 90.6%	98.7% 88%	DRIHSTHI
8	Sreng et al., 2020	modified DeepLabv3+	Deep learning	Accuracy	86.8%	--	DRISHTHI-GS1
9	Krishna Adithya et al., 2021	EffUnet+ResNet-Unet	Deep learning (Joint cup and disc)	Jaccard index Dice score Accuracy	85.4% 91.6% 99.68%	–	ORIGA DRISHTHI
10	Liu et al., 2019	GD-CNN	Deep Learning	Sensitivity	97.8%	92.2%	DRISHTHI-GS1
11	P. et al., 2021	Au-Net	Deep learning	Accuracy Sensitivity Specificity	99% 87% 92%	99% 86% 95%	DRISHTI-GS
12	Ganesh et al., 2021	GD-YNet	Deep learning	Accuracy Sensitivity Specificity	99.8% 98.1% 98.1%	–	DRISHTHI-GS1

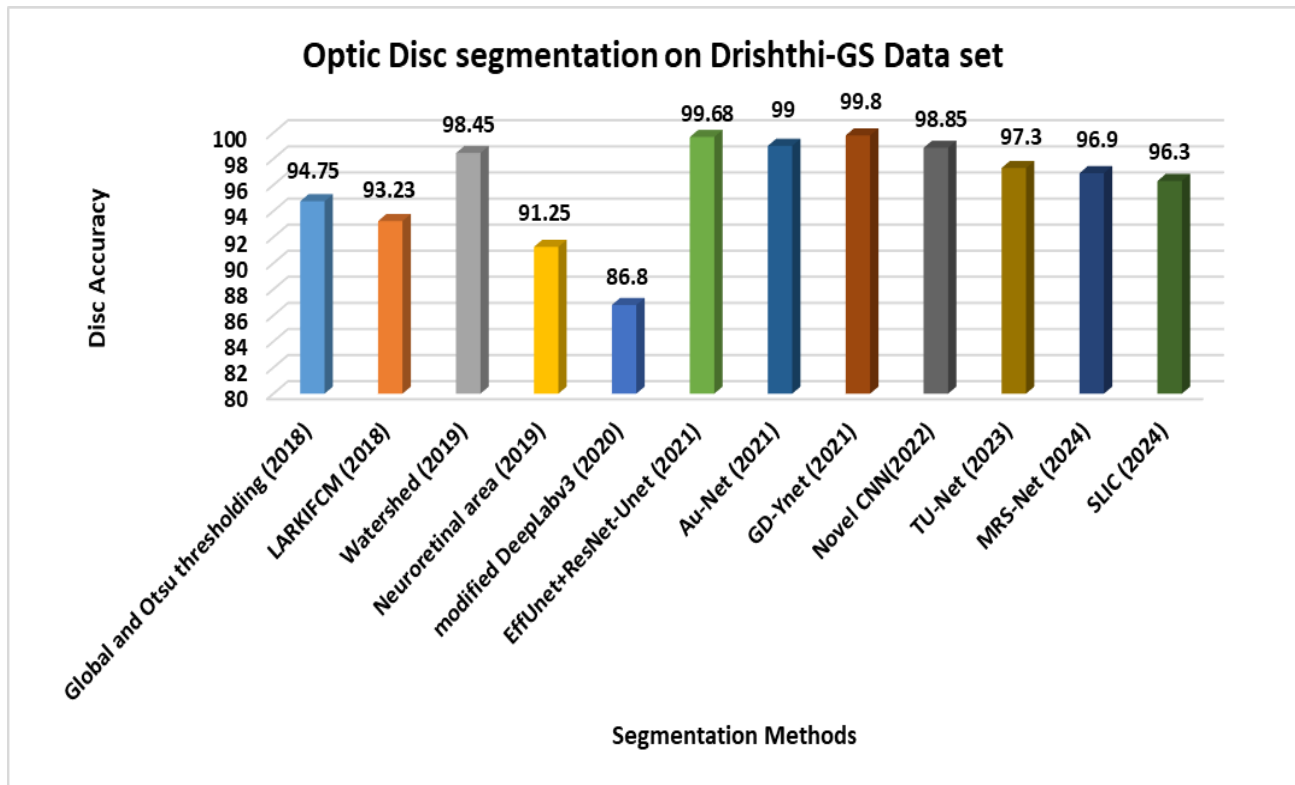| 13	Mayya et al.(2022)	Novel CNN	Deep Learning	Accuracy	98.55%	97.3%	DRISHT HI-GS1
14	Li et al., 2023)	TU-Net	Deep Learning	Accuracy	97.3%	90.3%	DRISHT HI-GS1
15	Yan et al., 2024	MRS-Net	Deep Learning	Accuracy	96.9%	85.9%	DRISHT HI-GS1
16	Diaz-Pinto et al., 2019	Residual Attention U-Net and U-Net++	Deep Learning	Dice score	97.9% 97.5%	87.7% 85.5%	DRISHT HI-GS1 RIM-ONE

Figure 5. Performance Analysis of Segmentation Approaches on DRISHTHI-GS Data set.

Conclusion and Future Scope

This paper provides a detailed analysis of various segmentation approaches utilized for the optic disc and optic cup segmentation from retinal fundus images. Different data sets of fundus images have been analyzed, and the study shows that most of the researchers have used the DRISHTHI-GS data set for optic disc segmentation, whereas limited research has been done on optic cup segmentation. The results provide high accuracy of the segmentation using deep learning-based techniques, but efficient computational techniques for optic disc and optic cup segmentation on complex data sets are still required. Variability in data set size, poor illumination, contrast, and image quality may not give a promising result using traditional deep learning techniques. Additionally, there is a problem of data imbalance that may lead to under-segmentation or over-segmentation. Innovative approaches are required to address all these challenges, which can robustly handle size variations, contrast issues, and the presence of interfering structures in retinal images. Future research efforts should prioritize using complex and large data sets, enhancing segmentation techniques and an efficient deep learning algorithm that can handle the variability and variety of the retinal image data set.

References

Al-Bander, B., Williams, B., Al-Nuaimy, W., Al-Taee, M., Pratt, H., & Zheng, Y. (2018). Dense Fully Convolutional Segmentation of the Optic Disc and Cup in Colour Fundus for Glaucoma Diagnosis. *Symmetry, 10*(4), 87. https://doi.org/10.3390/sym10040087

Almazroa, A. A., Alodhayb, S., Osman, E., Ramadan, E., Hummadi, M., Dlaim, M., Alkatee, M., Raahemifar, K., & Lakshminarayanan, V. (2018). Retinal fundus images for glaucoma analysis: The RIGA dataset. In J. Zhang & P.-H. Chen (Eds.), Medical Imaging 2018: *Imaging Informatics for Healthcare, Research, and Applications*, pp. 8. SPIE. https://doi.org/10.1117/12.2293584

Athab, S. D. (2019). Disc and cup segmentation for glaucoma detection. *Journal of Mechanics of Continua and Mathematical Sciences, 14*(6). https://doi.org/10.26782/jmcms.2019.12.00026

Bajwa, M. N., Singh, G. A. P., Neumeier, W., Malik, M. I., Dengel, A., & Ahmed, S. (2020).G1020: A Benchmark Retinal Fundus Image Dataset for Computer-Aided Glaucoma Detection (arXiv:2006.09158). arXiv. http://arxiv.org/abs/2006.09158

Chan, K. K. W., Tang, F., Tham, C. C. Y., Young, A. L., & Cheung, C. Y. (2017). Retinal vasculature in glaucoma: A review. *BMJ Open Ophthalmology, 1*(1), e000032. https://doi.org/10.1136/bmjophth-2016-000032

Chatterjee, S., Suman, A., Gaurav, R., Banerjee, S., Singh, A. K., Ghosh, B. K., Mandal, R. K., Biswas, M., & Maji, D. (2021). Retinal Blood Vessel Segmentation Using Edge Detection Method. *Journal of Physics: Conference Series, 1717*(1), 012008. https://doi.org/10.1088/1742-6596/1717/1/012008

Chaurasia, A., & Culurciello, E. (2017). LinkNet: Exploiting encoder representations for efficient semantic segmentation. *2017 IEEE Visual Communications and Image Processing* (VCIP), pp. 1–4. https://doi.org/10.1109/VCIP.2017.8305148

Coan, L. J., Williams, B. M., Krishna Adithya, V., Upadhyaya, S., Alkafri, A., Czanner, S., Venkatesh, R., Willoughby, C. E., Kavitha, S., & Czanner, G. (2023). Automatic detection of glaucoma via fundus imaging and artificial intelligence: A review. *Survey of Ophthalmology, 68*(1), 17–41. https://doi.org/10.1016/j.survophthal.2022.08.005

Delgado, M. F., Abdelrahman, A. M., Terahi, M., Miro Quesada Woll, J. J., Gil-Carrasco, F., Cook, C., Benharbit, M., Boisseau, S., Chung, E., Hadjiat, Y., & Gomes, J. A. (2019). Management Of Glaucoma In Developing Countries: Challenges And Opportunities For Improvement. *ClinicoEconomics and Outcomes Research, 11*, 591–604. https://doi.org/10.2147/CEOR.S218277

Diaz-Pinto, A., Morales, S., Naranjo, V., Köhler, T., Mossi, J. M., & Navea, A. (2019). CNNs for automatic glaucoma assessment using fundus images: An extensive validation. *BioMedical Engineering OnLine, 18*(1), 29. https://doi.org/10.1186/s12938-019-0649-y

Elyan, E., Vuttipittayamongkol, P., Johnston, P., Martin, K., McPherson, K., & Mostafa Kamal Sarker, Md. (2022). Computer vision and machine learning for medical image analysis: Recent advances, challenges, and way forward. *Artificial Intelligence Surgery.* https://doi.org/10.20517/ais.2021.15

Fu, H., Cheng, J., Xu, Y., Wong, D. W. K., Liu, J., & Cao, X. (2018). Joint Optic Disc and Cup Segmentation Based on Multi-label Deep Network and Polar Transformation. *IEEE Transactions on Medical Imaging, 37*(7), 1597–1605. https://doi.org/10.1109/TMI.2018.2791488

Fu, H., Cheng, J., Xu, Y., Zhang, C., Wong, D. W. K., Liu, J., & Cao, X. (2018). Disc-aware Ensemble Network for Glaucoma Screening from Fundus Image. *IEEE Transactions on Medical Imaging, 37*(11), 2493–2501. https://doi.org/10.1109/TMI.2018.2837012

Fu, H., Li, F., Orlando, J. I., Bogunović, H., Sun, X., Liao, J., Xu, Y., Zhang, S., & Zhang, X. (2019). REFUGE: Retinal Fundus Glaucoma Challenge [Dataset]. *IEEE DataPort.* https://doi.org/10.21227/TZ6E-R977

Fumero, F., Alayon, S., Sanchez, J. L., Sigut, J., & Gonzalez-Hernandez, M. (2011). RIM-ONE: An open retinal image database for optic nerve evaluation. *2011 24th International Symposium on Computer-Based Medical Systems* (CBMS), pp. 1–6. https://doi.org/10.1109/CBMS.2011.5999143

Gampala, V., Maram, B., Vigneshwari, S., & Cristin, R. (2022). Glaucoma detection using hybrid architecture based on optimal deep neuro fuzzy network. *International Journal of Intelligent Systems, 37*(9), 6305–6330. https://doi.org/10.1002/int.22845

Ganesh, S. S., Kannayeram, G., Karthick, A., & Muhibbullah, M. (2021). A Novel Context Aware Joint Segmentation and Classification Framework for Glaucoma Detection. *Computational and Mathematical Methods in Medicine, 2021*, 1–19. https://doi.org/10.1155/2021/2921737

Govindan, M., Dhakshnamurthy, V. K., Sreerangan, K., Nagarajan, M. D., & Rajamanickam, S. K. (2024). A Framework for Early Detection of Glaucoma in Retinal Fundus Images Using Deep Learning. *CC 2023*, 3. https://doi.org/10.3390/engproc2024062003

Gupta, N., Garg, H., & Agarwal, R. (2021). A robust framework for glaucoma detection using CLAHE and EfficientNet. The Visual Computer. https://doi.org/10.1007/s00371-021-02114-5

Ilesanmi, A. E., Ilesanmi, T., & Gbotoso, G. A. (2023). A systematic review of retinal fundus image segmentation and classification methods using convolutional neural networks. *Healthcare Analytics, 4*, 100261. https://doi.org/10.1016/j.health.2023.100261

Jiang, X., Zhang, R., & Nie, S. (2012). Image Segmentation Based on Level Set Method. Physics *Procedia, 33*, 840–845. https://doi.org/10.1016/j.phpro.2012.05.143

Juneja, M., Singh, S., Agarwal, N., Bali, S., Gupta, S., Thakur, N., & Jindal, P. (2020). Automated detection of Glaucoma using deep learning convolution network (G-net). *Multimedia Tools and Applications, 79*(21–22), 15531–15553. https://doi.org/10.1007/s11042-019-7460-4

Juneja, M., Thakur, S., Wani, A., Uniyal, A., Thakur, N., & Jindal, P. (2020). DC-Gnet for detection of glaucoma in retinal fundus imaging. *Machine Vision and Applications, 31*(5), 34. https://doi.org/10.1007/s00138-020-01085-2

Kauppi, T., Kalesnykiene, V., Kamarainen, J.-K., Lensu, L., Sorri, I., Raninen, A., Voutilainen, R., Uusitalo, H., Kalviainen, H., & Pietila, J. (2007). The DIARETDB1 diabetic retinopathy database and evaluation protocol. *Procedings of the British Machine Vision Conference, 15*, 1-15.10. https://doi.org/10.5244/C.21.15

Krishna Adithya, V., Williams, B. M., Czanner, S., Kavitha, S., Friedman, D. S., Willoughby, C. E., Venkatesh, R., & Czanner, G. (2021). EffUnet-SpaGen: An Efficient and Spatial Generative Approach to Glaucoma Detection. *Journal of Imaging, 7*(6), 92. https://doi.org/10.3390/jimaging7060092

Li, A., Winebrake, J. P., & Kovacs, K. (2023). Facilitating deep learning through preprocessing of optical coherence tomography images. *BMC Ophthalmology, 23*(1), 158. https://doi.org/10.1186/s12886-023-02916-2

Liu, H., Li, L., Wormstone, I. M., Qiao, C., Zhang, C., Liu, P., Li, S., Wang, H., Mou, D., Pang, R., Yang, D., Zangwill, L. M., Moghimi, S., Hou, H., Bowd, C., Jiang, L., Chen, Y., Hu, M., Xu, Y. Wang, N. (2019). Development and Validation of a Deep Learning System to Detect Glaucomatous Optic Neuropathy Using Fundus Photographs. *JAMA Ophthalmology, 137*(12), 1353. https://doi.org/10.1001/jamaophthalmol.2019.3501

M., S., Issac, A., & Dutta, M. K. (2018). An automated and robust image processing algorithm for glaucoma diagnosis from fundus images using novel blood vessel tracking and bend point detection. *International Journal of Medical Informatics, 110*, 52–70. https://doi.org/10.1016/j.ijmedinf.2017.11.015

Ma, X., Cao, G., & Chen, Y. (2024). A review of optic disc and optic cup segmentation based on fundus images. IET Image Processing, ipr2.13115. https://doi.org/10.1049/ipr2.13115

Maupin, E., Baudin, F., Arnould, L., Seydou, A., Binquet, C., Bron, A. M., & Creuzot-Garcher, C. P. (2020). Accuracy of the ISNT rule and its variants for differentiating glaucomatous from normal eyes in a population-based study. *British Journal of Ophthalmology, 104*(10), 1412–1417. https://doi.org/10.1136/bjophthalmol-2019-315554

Mayya, V., S, S. K., Kulkarni, U., Surya, D. K., & Acharya, U. R. (2023). An empirical study of preprocessing techniques with convolutional neural networks for accurate detection of chronic ocular diseases using fundus images. *Applied Intelligence, 53*(2), 1548–1566. https://doi.org/10.1007/s10489-022-03490-8

Medhi, J., Karmakar, M., Barman, A., Mondal, S., & Nag, A. (2023). Diabetic Retinopathy Stage Detection Using Convolutional Fine-Tuned Transfer Learning Model. *International Journal of Experimental Research and Review 31*(Spl Volume), 33-41. https://doi.org/10.52756/10.52756/ijerr.2023.v31spl.004.

Muchuchuti, S., & Viriri, S. (2023). Retinal Disease Detection Using Deep Learning Techniques: A Comprehensive Review. *Journal of Imaging, 9*(4), 84. https://doi.org/10.3390/jimaging9040084

Natarajan, D., Sankaralingam, E., Balraj, K., & Thangaraj, V. (2021). Automated segmentation algorithm with deep learning framework for early detection of glaucoma. *Concurrency and Computation: Practice and Experience, 33*(10), e6181. https://doi.org/10.1002/cpe.6181

Report of the 2030 targets on effective coverage of eye care. (2022). (World Health Organization) retrieved from Https://www.who.int/news-room/fact-sheets/detail/blindness-and-visual-impairment. (n.d.).

Rodriguez-Una, I., Febo., Azuara, B., Augusto., FRCOphth (2019). New Technologies for Glaucoma Detection. *Asia-Pacific Journal of Ophthalmology*. https://doi.org/10.22608/APO.2018349

P., S., J., R., & R., P. (2021). An automatic recognition of glaucoma in fundus images using deep learning and random forest classifier. *Applied Soft Computing, 109*, 107512. https://doi.org/10.1016/j.asoc.2021.107512

Pathan, S., Kumar, P., Pai, R. M., & Bhandary, S. V. (2021). Automated segmentation and classifcation of retinal features for glaucoma diagnosis. *Biomedical Signal Processing and Control, 63*, 102244. https://doi.org/10.1016/j.bspc.2020.102244

Rao, S. S., Ikram, S., & Ramesh, P. (2021). Deep Learning-Based Image Retrieval System with Clustering on Attention-Based Representations. *SN Computer Science, 2*(3), 179. https://doi.org/10.1007/s42979-021-00563-2

Rawat, S., & Kurmi, U. S. (2020). A Study on Glaucoma Disease Detection with Image Processing Methods. *Advanced Engineering Forum, 37*, 25–35. https://doi.org/10.4028/www.scientific.net/AEF.37.25

Ray, R., Jena, S., & Parida, P. (2022). An effective threshold-based technique for retinal image blood vessel segmentation using average & amp; Gaussian filters. https://doi.org/10.21203/rs.3.rs-1918836/v1

Saba, T., Bokhari, S. T. F., Sharif, M., Yasmin, M., & Raza, M. (2018). Fundus image classification methods for the detection of glaucoma: A review. *Microscopy Research and Technique, 81*(10), 1105–1121. https://doi.org/10.1002/jemt.23094

Saha, S., Vignarajan, J., & Frost, S. (2023). A fast and fully automated system for glaucoma detection using color fundus photographs. *Scientific Reports, 13*(1), 18408. https://doi.org/10.1038/s41598-023-44473-0

Sahu, D., & Kaur, M. (2021). Performance Analysis of Glaucoma Detection Techniques. 2021 *Fourth International Conference on Computational Intelligence and Communication Technologies* (CCICT), pp. 236–241. https://doi.org/10.1109/CCICT53244.2021.00052

Sanghavi, J., & Kurhekar, M. (2024). An efficient framework for optic disk segmentation and classification of Glaucoma on fundus images. *Biomedical Signal Processing and Control, 89*, 105770. https://doi.org/10.1016/j.bspc.2023.105770

Sevastopolsky, A. (2017). Optic disc and cup segmentation methods for glaucoma detection with modification of U-Net convolutional neural network. *Pattern Recognition and Image Analysis, 27*(3), 618–624. https://doi.org/10.1134/S1054661817030269

Shinde, R. (2021). Glaucoma detection in retinal fundus images using U-Net and supervised machine learning algorithms. *Intelligence-Based Medicine, 5*, 100038. https://doi.org/10.1016/j.ibmed.2021.100038

Shoukat, A., Akbar, S., Hassan, S. A. E., Rehman, A., & Ayesha, N. (2021). An Automated Deep Learning Approach to Diagnose Glaucoma using Retinal Fundus Images. 2021 *International Conference on Frontiers of Information Technology* (FIT), pp. 120–125. https://doi.org/10.1109/FIT53504.2021.00031

Sikder, N., Chowdhury, Md. S., Shamim Mohammad Arif, A., & Nahid, A.-A. (2019). Early Blindness Detection Based on Retinal Images Using Ensemble Learning. *2019 22ⁿᵈ International Conference on Computer and Information Technology* (ICCIT), pp. 1–6. https://doi.org/10.1109/ICCIT48885.2019.9038439

Singh, L. K., Pooja, P., & Garg, H. (2020). Detection of Glaucoma in Retinal Fundus Images using Fast Fuzzy C Mean Clustering. *International Journal of Fuzzy Systems and Advanced Applications, 7*, 16–23. https://doi.org/10.46300/91017.2020.7.4

Singh, P. B., Singh, P., & Dev, H. (2023). Optimized convolutional neural network for glaucoma detection with improved optic-cup segmentation. *Advances in Engineering Software, 175*, 103328. https://doi.org/10.1016/j.advengsoft.2022.103328

Sivapriya, G., & Keerthika, P. (2022). Computer aided diagnosis systems using deep learning for retinal diseases: A survey. *Materials Today: Proceedings, 58*, 286–292. https://doi.org/10.1016/j.matpr.2022.02.162

Sivaswamy, J., Krishnadas, S. R., Datt Joshi, G., Jain, M., & Syed Tabish, A. U. (2014). Drishti-GS: Retinal image dataset for optic nerve head(ONH) segmentation. *2014 IEEE 11th International Symposium on Biomedical Imaging* (ISBI), pp. 53–56. https://doi.org/10.1109/ISBI.2014.6867807

Sreng, S., Maneerat, N., Hamamoto, K., & Win, K. Y. (2020). Deep Learning for Optic Disc Segmentation and Glaucoma Diagnosis on Retinal Images. *Applied Sciences, 10*(14), 4916. https://doi.org/10.3390/app10144916

Staal, J., Abramoff, M. D., Niemeijer, M., Viergever, M. A., & Van Ginneken, B. (2004). Ridge-Based Vessel Segmentation in Color Images of the Retina. *IEEE Transactions on Medical Imaging, 23*(4), 501–509. https://doi.org/10.1109/TMI.2004.825627

Sujithra, B. S., & Albert Jerome, S. (2024). Adaptive cluster-based superpixel segmentation and BMWMMBO-based DCNN classification for glaucoma detection. *Signal, Image and Video Processing, 18*(1), 465–474. https://doi.org/10.1007/s11760-023-02751-4

Tadisetty, S., Chodavarapu, R., Jin, R., Clements, R. J., & Yu, M. (2023). Identifying the Edges of the Optic Cup and the Optic Disc in Glaucoma Patients by Segmentation. *Sensors, 23*(10), 4668. https://doi.org/10.3390/s23104668

Thakur, N., & Juneja, M. (2019). Optic disc and optic cup segmentation from retinal images using hybrid approach. *Expert Systems with Applications, 127*, 308–322. https://doi.org/10.1016/j.eswa.2019.03.009

Thakur, N., & Juneja, M. (2021). Early-stage prediction of glaucoma disease to reduce surgical requirements using deep-learning. Materials Today: *Proceedings, 45*, 5660–5664. https://doi.org/10.1016/j.matpr.2021.02.458

Tham, Y.-C., Li, X., Wong, T. Y., Quigley, H. A., Aung, T., & Cheng, C.-Y. (2014). Global Prevalence of Glaucoma and Projections of Glaucoma Burden through 2040. *Ophthalmology, 121*(11), 2081–2090. https://doi.org/10.1016/j.ophtha.2014.05.013

Yan, S., Pan, X., & Wang, Y. (2024). MRSNet: Joint consistent optic disc and cup segmentation based on large kernel residual convolutional attention and self-attention. *Digital Signal Processing, 145*, 104308. https://doi.org/10.1016/j.dsp.2023.104308

Yu, S., Xiao, D., Frost, S., & Kanagasingam, Y. (2019). Robust optic disc and cup segmentation with deep learning for glaucoma detection. *Computerized Medical Imaging and Graphics, 74*, 61–71. https://doi.org/10.1016/j.compmedimag.2019.02.0 05

Zahoor, M. N., & Fraz, M. M. (2017). Fast Optic Disc Segmentation in Retina Using Polar Transform. *IEEE Access, 5*, 12293–12300. https://doi.org/10.1109/ACCESS.2017.2723320

Zangalli, C., Gupta, S. R., & Spaeth, G. L. (2011). The disc as the basis of treatment for glaucoma. *Saudi Journal of Ophthalmology, 25*(4), 381–387. https://doi.org/10.1016/j.sjopt.2011.07.003

Zhuo Zhang, Feng Shou Yin, Jiang Liu, Wing Kee Wong, Ngan Meng Tan, Beng Hai Lee, Jun Cheng, & Tien Yin Wong. (2010). ORIGA-light: An online retinal fundus image database for glaucoma analysis and research. 2010 *Annual International Conference of the IEEE Engineering in Medicine and Biology*, pp. 3065–3068. https://doi.org/10.1109/IEMBS.2010.5626137